Relativistic DFT Studies of Dehydrogenation of Methane by Pt Cationic Clusters: Cooperative Effect of Bimetallic Clusters

Fei Xia and Zexing Cao*

Department of Chemistry and State Key Laboratory of Physical Chemistry of Solid Surfaces, Xiamen University, Xiamen 361005, China

Received: April 26, 2006; In Final Form: June 11, 2006

The dehydrogenation reaction mechanisms of methane catalyzed by transition-metal clusters PtM^+ (M = Cu, Ag, Au) and Pt_n^+ ($n = 2-4$) have been investigated theoretically. In the reactions of PtM^+ (M = Cu, Ag, Au) with CH_4, cleavage of the first C−H bond is quite facile without barrier. The second C−H bond activation and the release of H_2 from molecular complex are generally the rate-determining steps. In the reactions of platinum clusters Pt_n^+ ($n = 2-4$) with CH_4, the H_2 elimination from the dihydrogen complex is the rate-determining step. Spin crossover may occur in the reaction of Pt_2^+ and CH_4. Pt_2^+ and Pt_3^+ can dehydrogenate methane efficiently due to remarkable thermodynamic stability of the products. The dehydrogenation of methane induced by Pt_4^+ is less favored thermodynamically than Pt_n^+ ($n = 1, 2, 3$). On the basis of theoretical analyses, the differences in reactivity among the clusters and the nature of cooperative effect of the bimetallic cluster have been discussed. The calculated results provide a reasonable basis for understanding of experimental observations.

1. Introduction

The catalytic reactions mediated by transition-metal clusters have attracted considerable attention in recent years.[1−7] The intermediate-size clusters of transition metal as simplified models for study of heterogeneous catalysis might provide significant implication for the intrinsic mechanism of reaction on the surface. One of the most promising metals in catalytic applications is platinum, and it has been widely used for the inert C−H bond activation of methane.[3,8]

Early experimental studies by Cox and co-workers[9,10] show that methane can be efficiently activated by neutral Pt_n clusters ($n \leq 24$), and their reactivities vary with the cluster size. In particular, polyatomic clusters Pt_n ($n = 2-5$) are more reactive than single platinum atoms in dehydrogenation. Carroll et al.[11] calculated the potential energy curve of dehydrogenation reaction of a single Pt atom with methane, and they found that the most stable intermediate is a hydride $H-Pt-CH_3$, since the d^9s^1 configuration of Pt atom can accommodate two covalent bonds. The entire reaction is slightly endothermic by 7.2 kcal mol^{-1}, yielding the neutral carbene $PtCH_2$ and dihydrogen. Cui et al.[12,13] explored the C−H bond activation mechanism of methane by neutral platinum dimers and trimers theoretically. Their calculations indicate that neutral clusters Pt_2 and Pt_3 can activate the first C−H bond of methane with small barriers.

Alternatively, cationic clusters of transition metal exhibit relatively high reactivities in catalysis with respect to their neutral counterparts in the gas phase. Irikura et al.[14,15] found that methane can be spontaneously activated by the third-row metal ion Os^+, Ir^+, Pt^+, etc., yielding the metallic carbene cation and H_2. Such remarkable reactivities have been further elucidated by a series of experiments[16−23] in detail, in combination with theoretical calculations.[18,19,23] The overall reaction of Pt^+ and methane is calculated to be exothermic by 0.8 kcal mol^{-1} by the B3LYP approach.[19] Furthermore, Wesendrup et al.[24] noted that the bare Pt^+ cation catalyzes the reaction of methane with molecular oxygen to yield methanol, formaldehyde, and other oxygen-containing products. Aschi et al.[25] proposed a gas-phase model for the single Pt^+-catalyzed coupling of methane and ammonia to account for the industrial synthesis of hydrogen cyanide. In addition, small cationic platinum clusters can induce dehydrogenation of simple hydrocarbons.[26−28]

Recently, Achatz et al.[22] and Koszinowski et al.[16] have observed that methane could be dehydrogenated effectively by Pt_n^+ clusters ($n \leq 9$), giving rise to the species $Pt_nCH_2^+$ through the reaction $Pt_n^+ + CH_4 \rightarrow Pt_nCH_2^+ + H_2$, but there is an exception for the metal tetramer Pt_4^+. The reactivity of Pt_4^+ is sharply dropped to the minimum toward CH_4 among all cationic clusters, whereas the anionic Pt_4^- tetramer is relatively reactive. Interestingly, Koszinowski et al.[29,30] reported that the heteronuclear metal dimers PtM^+ (M = Cu, Ag, Au, Pt) are capable of efficiently dehydrogenating methane. The resulting metallic species $PtMCH_2^+$ (M = Cu, Ag, Au, Pt) should be taken as the important precursors to C−N bond coupling for the synthesis of HCN.[31−34]

Up to now, a few theoretical investigations have been performed on relatively small cationic platinum clusters.[35,36] A detailed understanding of such high reactivity of the cationic transition-metal clusters and its size dependence requires further theoretical investigations. In the present work, extensive relativistic DFT calculations on the dehydrogenation of methane by cationic metallic clusters PtM^+ (M = Cu, Ag, Au) and Pt_n^+ ($n = 2-4$) have been performed. Possible dehydrogenation mechanisms and reactivities have been discussed.

2. Computational Details

All calculations in the present work have been performed using the Amsterdam density-functional (ADF) package.[37−40] Since the relativistic effect[41,42] is important in these Pt-containing

* To whom correspondence should be addressed. E-mail: zxcao@xmu.edu.cn.

10.1021/jp062544e CCC: $33.50
Published on Web 07/28/2006

TABLE 1: A Comparison of Predicted and Experimental Internuclear Distances (R_e, Å) and Adiabatic Ionization Potential (AIP, eV) for Neutral Metal Dimers

species	property	BP86	BLYP	BPW91	exptl[51−55]
$Pt_2(^3\Sigma_g^-)$	R_e	2.3503	2.3786	2.3504	2.3329
	AIP	8.80	8.61	8.67	8.68
$PtCu(^2\Delta)$	R_e	2.3006	2.3395	2.3123	2.3353
	AIP	8.81	8.62	8.62	8.26
$CuAg(^1\Sigma^+)$	R_e	2.3978	2.4002	2.3983	2.3735
	AIP	8.29	8.19	8.04	7.78
$CuAu(^1\Sigma^+)$	R_e	2.3365	2.3684	2.3426	2.3302
	AIP	8.60	8.94	8.50	8.74

metal clusters, and the zero-order regular approximation formalism (ZORA) without the spin−orbit coupling has thus been used.[43,44] Previous studies[45] indicate that the BPW91 functional with the ZORA approximation can predict reliable properties of metal dimers in comparison with the Dirac four-component-MP2 calculations.[46] As Table 1 shows, the calculated equilibrium internuclear distances and adiabatic ionization potentials (AIPs) of neutral metal dimers by the gradient-corrected functionals BP86,[47,48] BLYP,[47,49] and BPW91[47,50] are reasonably in agreement with available experiments.[51−55] The BPW91 dissociation energy of Pt_2 is 3.67 eV, higher than the experimental value by about 0.5 eV,[56] but it is comparative with the sophisticated CASPT2 treatments.[12] These test calculations indicate that the BPW91-optimized geometrical parameters have an accuracy of no more than 0.02 Å and the predicted relative energies have a deviation within 0.5 eV in comparison with experiments. The BPW91 functional has thus been employed here.

In calculation, the 1s-2p orbitals for Cu, 1s-3d orbitals for Ag, 1s-4f orbitals for Au and Pt, and 1s orbitals for C and N are kept frozen respectively in the frozen core approximation. The valence orbitals based on the Slater-type orbital are expanded within the triple-ζ basis set augmented with two polarization functions. Frequency analyses have been used to assess the nature of intermediates and transition states. Calculated zero-point energy corrections have been incorporated into total energies. In addition, the constrained optimization is used to execute the potential energy scan, which might make it easier to search the possible complexes of methane and metal clusters.

In consideration of spin flip[57−59] in reaction, these transition-metal species with different spin multiplicity have been optimized. The effect of spin crossover on the reaction mechanism was discussed.

3. Results and Discussion

3.1. Reactions of PtM^+ (M = Cu, Ag, Au) and CH_4. Theoretical studies of the heteronuclear bimetallic PtM (M = Cu, Ag, Au) clusters are relatively scarce.[60−62] Previous calculations by Dai et al.[60] reveal that the ground state of the cationic $PtAu^+$ cluster is $^1\Sigma^+$ with a valence electron configuration of $1\sigma^2 2\sigma^2 1\pi^4 1\pi^4 1\delta^4 2\delta^4$. Similarly, present relativistic DFT calculations show that these cationic bimetallic clusters PtM^+ (M = Cu, Ag, Au) have the same ground states of $^1\Sigma^+$.

Among mononuclear cations M^+ (M = Pt, Cu, Ag, Au), the oxidation addition catalyzed by Pt^+ constitutes the first step in the dehydrogenation reaction of methane,[59,63,64] whereas other metal cations are inactive toward CH_4 due to relatively weak metal−carbon bonds and closed-shell structures in their ground states. Generally, the methane activation to MCH_2^+ requires a metal−carbene bond strength of 111.0 kcal mol^{-1} thermodynamically.[65,66] For Au^+, the reactive excited state of $d^9s^1(^3D_3)$ as a precursor to Au−H and Au−C couplings is higher in energy than the ground state of d^{10} ($^1S_0$) by 43.0 kcal mol^{-1}.[14,15] Therefore, the reactive states of Au^+, as well as Ag^+ and Cu^+, are less accessible energetically, and the terminal Pt with an open d subshell configuration in these bimetallic cationic clusters should have relatively high activity. Further calculations show that the hydride $Pt-M(CH_3)H^+$ from C−H activation at the M site (M = Cu, Ag, Au) is less stable than $M-Pt(CH_3)H^+$. For example, $Pt-Au(CH_3)H^+$ is 20 kcal mol^{-1} above $Au-Pt(CH_3)H^+$. The terminal Pt is thus considered as the initial active site for the first C−H bond activation of methane.

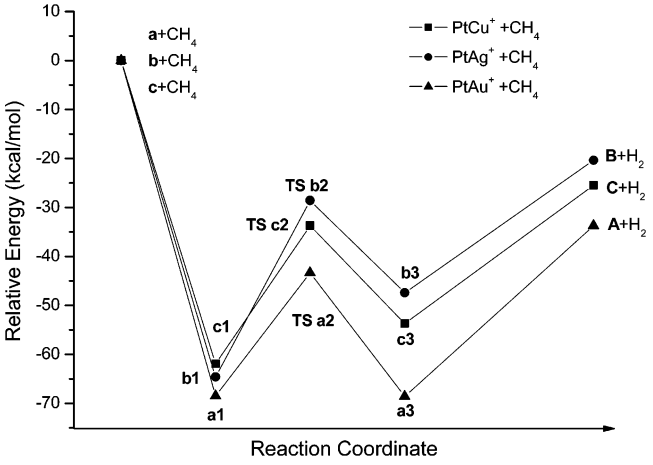

Figure 1. Potential energy profiles of reactions of PtM^+ (M = Cu, Ag, Au, Pt) and CH_4.

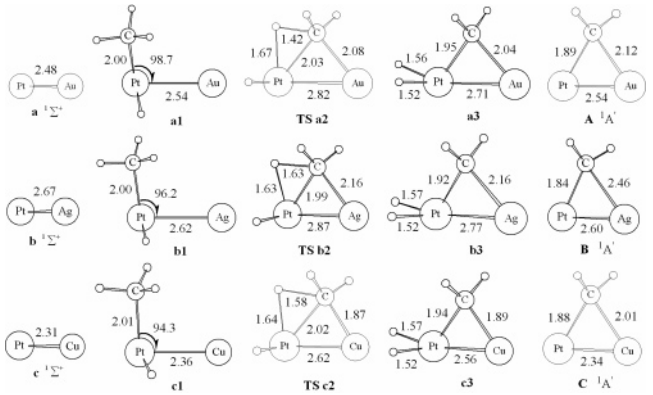

Figure 2. Optimized structures of transition states and intermediates corresponding to Figure 1 (bond lengths in angstroms and bond angles in degrees).

Figure 1 presents relative energy profiles of reactions of PtM^+ (M = Cu, Ag, Au) with methane. Corresponding geometries and thermodynamic values of selected species in reaction are shown in Figure 2 and Table 2, respectively. As shown in Table 2 and Figure 2, the formation of additive products $AuPt(CH_3)H^+$ (**a1**), $AgPt(CH_3)H^+$ (**b1**), and $CuPt(CH_3)H^+$ (**c1**) releases an energy of 68.5, 64.6, and 63.2 kcal mol^{-1}, respectively. Detailed potential energy surface scans reveal that the first C−H activation of methane mediated by these cationic clusters is barrier free to yield the hydride complexes. Followed by the second C−H activation, the stable intermediates $(H)_2Pt(\mu\text{-}CH_2)Au^+$(**a3**), $(H)_2Pt(\mu\text{-}CH_2)Ag^+$(**b3**), and $(H)_2Pt(\mu\text{-}CH_2)Cu^+$(**c3**) are formed through transition states **TS a2**, **TS b2**, and **TS c2**, respectively. Corresponding barriers are 25.2, 36.0, and 28.1 kcal mol^{-1}, respectively. Such transition states have been confirmed by further frequency analyses and IRC[67,68] calculations.

The elimination of dihydrogen in the intermediates **a3**, **b3**, and **c3** requires energies of 34.9, 27.0, and 28.2 kcal mol^{-1},

TABLE 2: The Calculated Thermodynamic Values (kcal mol^{-1}) at 298.15 K of Species in the Reactions of PtM$^+$ (M = Cu, Ag, Au) with CH_4

species	$\Delta E°$	$\Delta H°$	$\Delta G°$	species	$\Delta E°$	$\Delta H°$	$\Delta G°$
a + CH_4	0.0	0.0	0.0	**c** + CH_4	0.0	0.0	0.0
a1	−68.5	−68.9	−61.6	**c1**	−63.2	−63.1	−56.0
TS a2	−43.3	−44.2	−35.9	**TS c2**	−35.1	−35.3	−27.1
a3	−68.6	−69.4	−61.0	**c3**	−55.0	−55.2	−47.0
A + H_2	−33.7	−33.1	−32.7	**C** + H_2	−26.8	−25.5	−25.4
b + CH_4	0.0	0.0	0.0				
b1	−64.6	−65.2	−57.5				
TS b2	−28.6	−29.5	−20.9				
b3	−47.4	−48.3	−39.5				
B + H_2	−20.4	−19.5	−19.8				

respectively, yielding bimetallic carbenes Pt(μ-CH_2)Au$^+$ (**A**), Pt(μ-CH_2)Ag$^+$ (**B**), and Pt(μ-CH_2)Cu$^+$ (**C**). These products as precursors can react with ammonia,[29−34,45] giving rise to C−N coupling and consecutive hydrogenation. Unlike the case of methane activation by Pt$^+$,[18,19] no stable dihydrogen complex was found in calculation. The overall hydrogenation reactions catalyzed by the cationic PtM$^+$ clusters (M = Au, Ag, Cu) have free energies of reaction ΔG of −32.7, −19.8, and −25.4 kcal mol^{-1}.

3.2. Reactions of Pt_2^+ and CH_4. A number of theoretical calculations have been carried out for Pt_2.[12,56,69−71] The neutral Pt_2 cluster has a triplet ground state of $^3\Sigma_g^-$. As Table 1 displays, the $X^3\Sigma_g^-$ state has a bond length of 3.350 Å and an adiabatic ionization potential of 8.67 eV by BPW91, which are in good agreement with experimental values.[52] The cationic Pt_2^+ cluster was predicted to have a quartet ground state of $^4\Sigma_u^-$, and the next stable doublet state $^2\Sigma_u^-$ is 7.2 kcal mol^{-1} above the ground state.[35] Since both states have comparable stabilities, they can serve as initial states of Pt_2^+ in the dehydrogenation reaction. Figure 3 displays the relative energy profiles for the reaction of Pt_2^+ and CH_4 on the doublet and quartet potential energy surfaces. Optimized structures and thermodynamic values of species in reaction are shown in Figure 4 and Table 4, respectively.

Figure 3 displays two plausible mechanisms for dehydrogenation of methane mediated by Pt_2^+. In the quartet route, formation of the molecule−ion complex $Pt_2(CH_4)^+$ (**^{4}d1**) releases an energy of 20.1 kcal mol^{-1}. The complex **^{4}d1** proceeds to a hydride intermediate PtPt(CH_3)H$^+$ (**^{4}d3**) via the C−H bond activation with a barrier of 7.4 kcal mol^{-1}. Followed by the second C−H bond activation and association of two

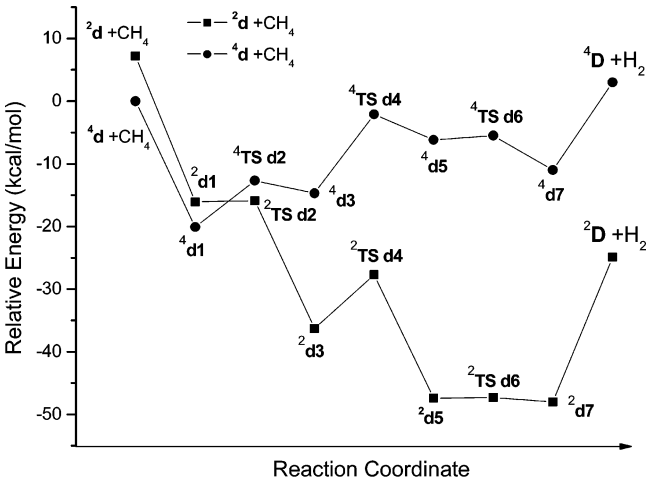

Figure 3. Potential energy profiles of reactions of CH_4 and Pt_2^+ in quartet and doublet states.

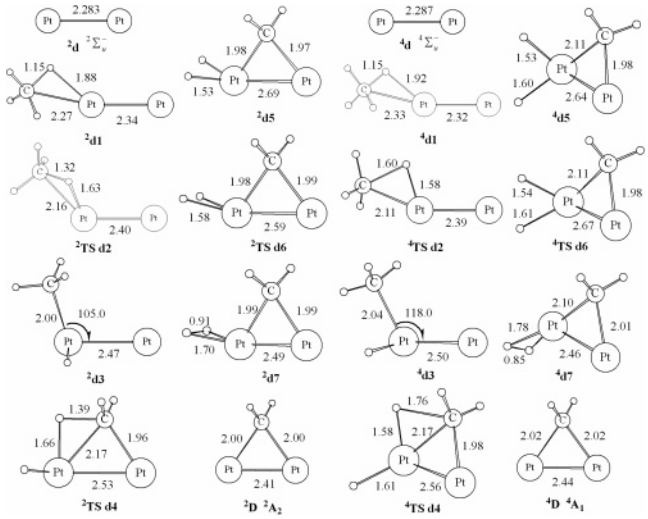

Figure 4. Optimized structures of transition states and intermediates corresponding to Figure 3 (bond lengths in angstroms and bond angles in degrees).

TABLE 3: Mulliken Populations of PtM$^+$ (M = Cu, Ag, Au) and Pt_n^+ (n = 2−4)

species	atoms	Mulliken populations	species	atoms	Mulliken populations
$PtAu^+$	Pt	$6s^{0.48}\,5d^{8.82}\,6p^{0.06}$	$^2Pt_2^+$	Pt	$6s^{0.99}\,5d^{8.38}\,6p^{0.08}$
	Au	$6s^{0.81}\,6d^{9.68}\,6p^{0.08}$	$^4Pt_2^+$	Pt	$6s^{0.99}\,5d^{8.39}\,6p^{0.08}$
$PtAg^+$	Pt	$6s^{0.25}\,5d^{9.25}\,6p^{0.04}$	$^2Pt_3^+$	Pt	$6s^{0.77}\,5d^{8.71}\,6p^{0.13}$
	Ag	$5s^{0.39}\,4d^{9.95}\,5p^{0.08}$	$^2Pt_4^+$	Pt1, Pt2	$6s^{0.71}\,5d^{8.77}\,6p^{0.19}$
$PtCu^+$	Pt	$6s^{0.54}\,5d^{8.88}\,6p^{0.02}$		Pt3, Pt4	$6s^{0.67}\,5d^{8.89}\,6p^{0.17}$
	Cu	$6s^{0.64}\,5d^{9.70}\,6p^{0.12}$	$^4Pt_4^+$	Pt	$6s^{0.68}\,5d^{8.84}\,6p^{0.17}$
Pt^+	Pt	$6s^0\,5d^9$			

TABLE 4: The Calculated Thermodynamic Values (kcal mol^{-1}) at 298.15 K of the Reaction of Pt_2^+ with CH_4 in Doublet and Quartet States

species	$\Delta E°$	$\Delta H°$	$\Delta G°$	species	$\Delta E°$	$\Delta H°$	$\Delta G°$
^{2}d + CH_4	7.2	9.2	9.2	**^{4}d** + CH_4	0.0	0.0	0.0
^{2}d1	−16.1	−16.7	−9.2	**^{4}d1**	−20.1	−20.6	−14.3
^{2}TS d2	−15.9	−16.6	−9.3	**^{4}TS d2**	−12.7	−13.1	−6.1
^{2}d3	−36.3	−36.8	−29.9	**^{4}d3**	−14.7	−15.0	−8.5
^{2}TS d4	−27.7	−28.5	−20.5	**^{4}TS d4**	−2.1	−2.9	5.0
^{2}d5	−47.4	−48.1	−40.7	**^{4}d5**	−6.2	−6.8	0.7
^{2}TS d6	−47.3	−48.2	−39.9	**^{4}TS d6**	−5.5	−5.8	0.3
^{2}d7	−48.0	−48.8	−40.7	**^{4}d7**	−11.0	−11.7	−3.9
^{2}D + H_2	−24.9	−24.4	−23.7	**^{4}D** + H_2	3.0	3.5	4.0

hydrogen atoms, the molecular complex (H_2)Pt(μ-CH_2)Pt$^+$ (**^{4}d7**) is formed. The loss of H_2 in the complex **^{4}d7** requires an energy of 14.0 kcal mol^{-1}, giving rise to products Pt(μ-CH_2)Pt$^+$ (**^{4}D**) and H_2. The overall reaction on the potential energy surface of the quartet state has free energies of reaction ΔG of 4.0 kcal mol^{-1}.

The reaction in the doublet pathway follows the same mechanism with the quartet state. The doublet reaction is significantly exothermic by 32.1 kcal mol^{-1}. The free energies of reaction ΔG is −32.9 kcal mol^{-1}. As Figure 3 shows, the reactive species is likely to change its spin multiplicity from the quartet state to the doublet state in reaction.[59] The lowest-cost reaction pathway will start from the quartet state. Followed by the first C−H bond activation, the quartet molecular complex $Pt_2(CH_4)^+$ (**^{4}d1**) may evolve into the doublet intermediate PtPt-(CH_3)(H)$^+$ (**^{2}d3**) with spin flip. Subsequent to consecutive isomerizations and elimination of H_2, the reaction gives the doublet product Pt(μ-CH_2)Pt$^+$ (**^{2}D**). The loss of H_2 from the molecular complex (H_2)Pt(μ-CH_2)Pt$^+$ (**^{2}d7**) as a rate-determining step requires 23.1 kcal mol^{-1}. The spin transition here will

SCHEME 1: The HOMOs and LUMOs of CH_4 and $PtAu^+$

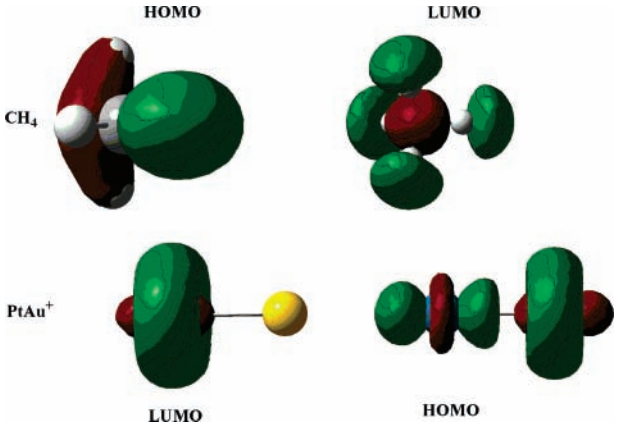

enhance the reactivity of Pt_2^+. This is consistent with the experimental finding that Pt_2^+ is more efficient than single Pt^+ in dehydrogenating methane.[16,22] The effects of spin flip on the gas-phase ion−molecule reactions have been reviewed by Schwarz.[59]

3.3. Electronic Structure and Reactivity of Pt^+ and PtM^+. As illuminated by experimental studies, the calculated results indicate that the bimetallic clusters PtM^+ (M = Cu, Ag, Au, Pt) exhibit dissimilar reactivity with the single Pt^+. Generally, the bimetallic clusters exhibit higher activity toward CH_4 activation with respect to Pt^+. The remarkable reactivity of heteronuclear clusters PtM^+ (M = Cu, Ag, Au) toward first C−H activation can be understood through the frontier orbital interaction and the simple donor−acceptor model.[72,73] As Scheme 1 displays, when CH_4 approaches to $PtAu^+$, the lowest unoccupied molecular orbital (LUMO) of $PtAu^+$ and the C−H bonding orbital of CH_4 have the same phase patterns and these phase-adaptation frontier orbitals can efficiently interact to activate the C−H bond. Note that the highest occupied molecular orbital (HOMO) of $PtAu^+$ is mainly from Au, and thus the presence of Au will enhance interaction between the HOMO and the σ^* orbital (LUMO) of CH_4 with respect to single Pt^+. The cooperative bonding interactions in the complex of $PtAu^+$ with CH_4, where the metal cationic cluster behaves as an acceptor to reduce bonding electrons in the C−H σ bond and it also behaves as a donor to increase antibonding electrons in the C−H σ^* bond of methane, result in the cleavage of the C−H bond. For other PtM^+/CH_4 systems, there are similar orbital interaction mechanisms for the C−H bond activation.

Similarly, such cooperative bonding interactions among the frontier orbitals of bimetallic clusters and the H−H σ and σ^* orbitals will make the dihydrogen complexes of PtM^+ (M = Cu, Ag, Au) unstable, and thus no stable molecular complexes of H_2 have been found in the dehydrogenation of CH_4 as DFT calculations show.

Mulliken atom populations in Table 3 reveal that the platinum in PtM^+ (M = Cu, Ag, Au) has an approximate $5d^9$ configuration similar to Pt^+, and Cu, Ag, and Au have an approximate $(n-1)d^{10}$ structure and partial *n*s populations. Such almost closed d subshell configurations suggest that the Cu, Ag, and Au terminals are inert toward methane in their ground states. Thus the terminal platinum with the open d subshell in PtM^+ is still the active site for the C−H bond activation.

Mulliken populations of Pt_2^+ display that the platinum in the doublet and quartet states has an approximate s^1d^8 configuration with three unpaired electrons, similar to the excited Pt^+ cation. Such active electronic structure of Pt in Pt_2^+ is able to form

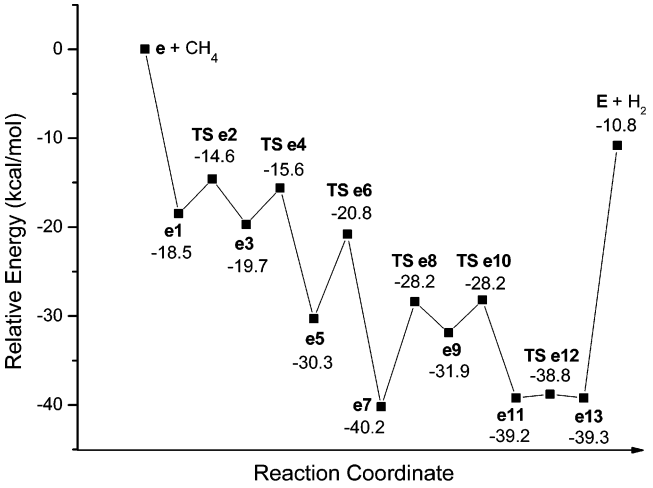

Figure 5. Potential energy profile of reaction of Pt_3^+ and CH_4.

three covalent bonds and may facilitate the second C−H bond activation with a low barrier of 8.6 kcal mol^{-1} as shown in Figure 3. This consecutive C−H activation energy in $PtPt(CH_3)H^+$ (**^{2}d3**) is much smaller than the corresponding barriers of 28.1 for $CuPt(CH_3)H^+$ (**c1**), 36.0 for $AgPt(CH_3)H^+$ (**b1**), and 25.2 kcal mol^{-1} for $AuPt(CH_3)H^+$ (**a1**), respectively.

3.4. Reactions of Pt_n^+ (n = 3, 4) and CH_4. The relative energy profiles of reaction of Pt_3^+ with CH_4 are shown in Figure 5, and the corresponding structures of species in reactions are displayed in Figure 6. The most stable structure **e** of the trimer is an equilateral triangle in D_{3h} symmetry as shown by the previous calculation.[35] The Pt−Pt separation in the ground state $^2A_1''$ is 2.45 Å.

The formation of complex $Pt_3(CH_4)^+$ (**e1**) of **e** with CH_4 has an exothermicity of 18.5 kcal mol^{-1}, which is agreement with the previous predicted binding energy of 16.6 kcal mol^{-1}.[36] An effort to locate other isomers of the complex $Pt_3(CH_4)^+$ has been made, and only an isoenergetic analogue of **e1** has been found. Cleavage of the first C−H bond gives rise to the intermediate **e3** with a small barrier of 3.9 kcal mol^{-1}. Through consecutive hydrogen transfers, **e3** evolves to the more stable isomer **e7**. The intermediate **e7** undergoes the second C−H bond activation with a barrier of 12.0 kcal mol^{-1} and intramolecular isomerizations, yielding a dihydrogen complex **e13**. The molecular complex **e13** require 28.5 kcal mol^{-1} to release H_2, yielding the product **E**. As Figure 5 displays, the loss of dihydrogen is the rate-determining step for the reaction of Pt_3^+ with CH_4. The entire reaction has an exothermicity of 10.8 kcal mol^{-1} and reaction free energy ΔG of −8.9 kcal mol^{-1}.

The doublet and quartet potential energy profiles of the reaction of Pt_4^+ with CH_4 are shown in Figure 7. The corresponding structures of species in reactions are displayed in Figure 8. The Pt_4^+ tetramer has been predicted to be a stable tetrahedral structure (**^{4}f**) in T_d symmetry.[35] The lowest-energy state $^4A_1$ arises from an electronic configuration of $a_1^4e^8t_2^{18}t_1^6t_1^3$. The next stable doublet state $^2A_2$ has a stable C_{2v} structure (**^{2}f**), which is less stable than the quartet state **^{4}f** by 6.5 kcal mol^{-1}.

On the quartet potential energy surface, the formation of complex **^{4}f1** of Pt_4^+ with CH_4 releases an energy of 14.5 kcal mol^{-1}. In full geometry optimization, distinct initial structures of the complex $Pt_4(CH_4)^+$ evolve to **^{4}f1** or its analogue with the same Pt···(CH_4) coordination. The isoenergetic isomers arise from internal rotation of the distal Pt_3 subunit around Pt···(CH_4). Followed by cleavage of the first C−H bond and hydrogen migration, a less stable intermediate **^{4}f5** is generated. The intermediate **^{4}f5** requires 3.3 kcal mol^{-1} to yield **^{4}f6**. **^{4}f6** proceeds

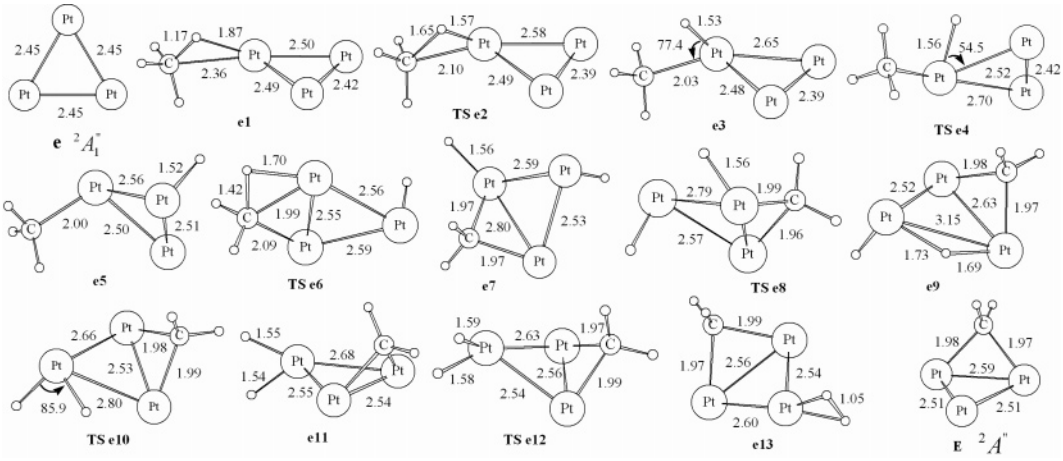

Figure 6. Optimized structures of transition states and intermediates corresponding to Figure 5 (bond lengths in angstroms and bond angles in degrees).

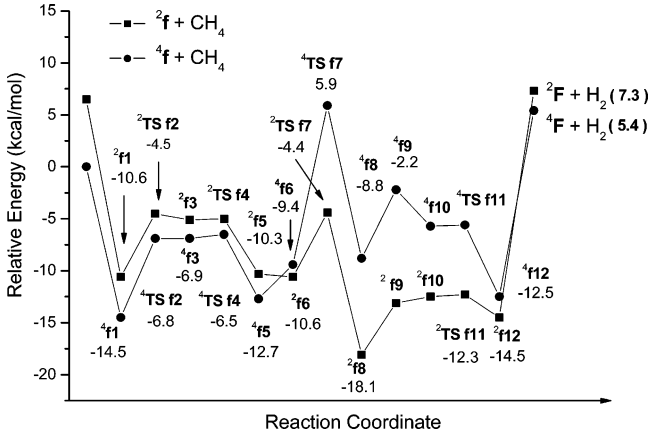

Figure 7. Potential energy profiles of reactions of methane and Pt_4^+ in quartet and doublet states.

to **^{4}f8** through the transition state **^{4}TS f7** with a barrier of 15.3 kcal mol^{-1}. The intermediate **^{4}f8** evolves to the dihydrogen complex **^{4}f12** via hydrogen shifts. The release of H_2 from **^{4}f12** requires 17.9 kcal mol^{-1}. The overall reaction on the quartet potential energy surface is slightly endothermic by 5.4 kcal mol^{-1}, and the calculated free energy of the entire reaction ΔG is 6.7 kcal mol^{-1}.

As Figure 7 shows, the reaction on the doublet potential energy surface follows similar mechanisms with the quartet state. The overall reaction is endothermic by 7.3 kcal mol^{-1}. Note that the spin transition from the quartet to doublet state is probably involved in the hydrogen transfer process from **^{4}f5** to **^{4}f6**. The spin transition from **^{4}f6** to the more stable **^{2}f6** will significantly lower the barrier height for the second C−H bond activation.

Unlike Pt_2^+ and Pt_3^+, the dehydrogenation of CH_4 by Pt_4^+ has a reaction free energy ΔG of 6.7 kcal mol^{-1}. Thus the overall reaction of Pt_4^+ with CH_4 is not favorable thermodynamically. The calculated results support the experimental finding that Pt_4^+ has an anomalously reactivity toward dehydrogenation of CH_4 with respect to other Pt_n^+ (n = 1, 2, 3, 5).[16,22] However, predicted barriers are generally low and the reaction may be favored dynamically. Once the insufficient thermodynamic drive is compensated, the reactivity will be improved strikingly as observed experimentally.[28]

Contrary to the dehydrogenation process, the reverse reaction: $Pt_4CH_2^+ + H_2 \rightarrow Pt_4^+ + CH_4$ should be facile thermodynamically as shown in Figure 7, and the barriers of the rate-determining steps are less than 15 kcal mol^{-1} in the formation of methyl group. Experimentally, the reverse reaction was

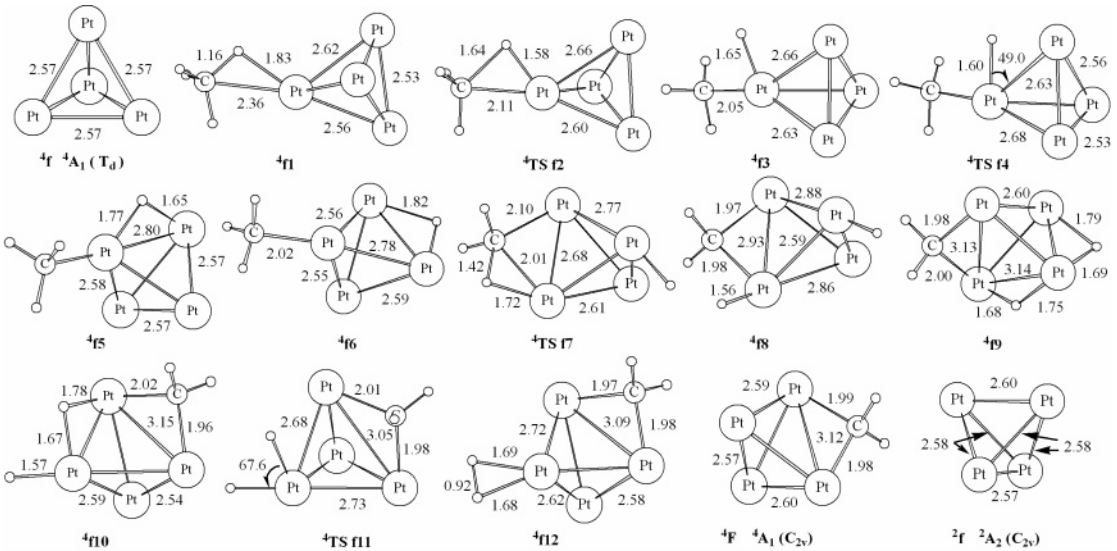

Figure 8. Optimized structures of transition states and intermediates corresponding to Figure 7 (bond lengths in angstroms and bond angles in degrees).

observed for $Pt_4CH_2^+$,[16] whereas the other species $Pt_nCH_2^+$ ($n = 2,3$) do not react with H_2.

4. Conclusions

Relativistic DFT calculations have been used to explore reactivity of the metal cationic clusters PtM^+ (M = Cu, Ag, Au) and Pt_n^+ ($n = 2-4$) toward methane. Our calculations show that the spin multiplicity might change in the lowest-cost dehydrogenation process of methane by Pt_2^+. The spin transition may significantly enhance the reactivity. When one of Pt atom in Pt_2^+ is replaced by the inert metal M (M = Cu, Ag, Au), the reactivity of PtM^+ (M = Cu, Ag, Au) toward methane is less changed, and the terminal Pt in PtM^+ (M = Cu, Ag, Au) is the preferred site for C−H activation. The cooperative effect of the bimetallic cluster may facilitate the first C−H activation with respect to Pt^+.

In the reactions of Pt_3^+ and Pt_4^+ clusters with methane, the final steps of H_2 elimination are the rate-determining steps. In comparison with Pt_3^+, Pt_4^+ exhibits relatively low reactivity due to the lack of thermodynamic stability of the product. However, the dynamical feasibility makes the dehydrogenation of methane catalyzed by Pt_4^+ practicable with the increase of kinetic energy as observed experimentally.

Acknowledgment. We thank Dr. G. B. Zhang for participating in the discussion and acknowledge financial support from the National Science Foundation of China (Projects 20173042, 20233020, 20473062, and 20021002), the Ministry of Education of China, and the Ministry of Science and Technology (Projects 2004CB719902 and 001CB1089).

References and Notes

(1) Bond, G. C. In *Chemistry of the Platinum Group Metals: Recent Developments*; Hartley, F. R., Ed.; Elsevier: Amsterdam, 1991; Chapter 2.

(2) Sinfelt, J. H. In *Catalysis: Science and Technology*; Anderson, J. R., Boudart, M., Eds.; Springer-Verlag: Heidelberg, 1981; Vol. 1, Chapter 5.

(3) Eller, K.; Schwarz, H. *Chem. Rev.* **1991**, *91*, 1121.

(4) Thomas, J. M. *Angew. Chem., Int. Ed. Engl.* **1994**, *33*, 913.

(5) Schwarz, H.; Schröder, D. *Pure Appl. Chem.* **2000**, *72*, 2319.

(6) Balaj, O. P.; Balteanu, I.; Rossteuscher, T. T. J.; Beyer, M. K. Bondybey, V. E. *Angew. Chem., Int. Ed.* **2004**, *43*, 6519.

(7) Balteanu, I.; Balaj, O. P.; Beyer, M. K.; Bondybey, V. E. *Phys. Chem. Chem. Phys.* **2004**, *6*, 2910.

(8) Lersch, M.; Tilset, M. *Chem. Rev.* **2005**, *105*, 2471.

(9) Trevor, D. J.; Cox, D. M.; Kaldor, A. *J. Am. Chem. Soc.* **1990**, *112*, 3742.

(10) Kaldor, D. A.; Cox, D. M. *Pure Appl. Chem.* **1990**, *62*, 79.

(11) Carroll, J. J.; Weisshaar, J. C. *J. Chem. Phys.* **1995**, *99*, 14388.

(12) Cui, Q.; Musaev, D. G.; Morokuma, K. *J. Chem. Phys.* **1998**, *180*, 8418.

(13) Cui, Q.; Musaev, D. G.; Morokuma, K. *J. Phys. Chem. A* **1998**, *102*, 6373.

(14) Irikura, K. K.; Beauchamp, J. L. *J. Am. Chem. Soc.* **1991**, *113*, 2769.

(15) Irikura, K. K.; Beauchamp, J. L. *J. Phys. Chem.* **1991**, *95*, 8344.

(16) Koszinowski, K.; Schröder, D.; Schwarz, H. *J. Phys. Chem. A* **2003**, *107*, 4999.

(17) Heinemann, C.; Hertwig, R.; Wesendrup, R.; Koch, W.; Schwarz, H. *J. Am. Chem. Soc.* **1995**, *117*, 495.

(18) Heinemann, C.; Wesendrup, R.; Schwarz, H. *Chem. Phys. Lett.* **1995**, *239*, 75.

(19) Pavlov, M.; Bomberg, M. R. A.; Seigbahn, P. E. M.; Wesendrup, R.; Heinemann, C.; Schwarz, H. *J. Phys. Chem. A* **1997**, *101*, 1567.

(20) Taylor, W. S.; Campbell, A. S.; Barnas, D. F.; Babcock, L. M.; Linder, C. B. *J. Phys. Chem. A* **1997**, *101*, 2654.

(21) Achatz, U.; Beyer, M.; Joos, S.; Fox, B. S.; Niedner-Schatteburg, G.; Bondybey, V. E. *J. Phys. Chem. A* **1999**, *103*, 8200.

(22) Achatz, U.; Berg, C.; Joos, S.; Fox, B. S.; Beyer, M. K.; Niedner-Schatteburg, G.; Bondybey, V. E. *Chem. Phys. Lett.* **2000**, *320*, 53.

(23) Zhang, X. G.; Liyanage, R.; Armentrout, P. B. *J. Am. Chem. Soc.* **2001**, *123*, 5563.

(24) Wesendrup, R.; Schröder, D.; Schwarz, H. *Angew. Chem., Int. Ed. Engl.* **1994**, *33*, 1174.

(25) Aschi, M.; Brönstrup, M.; Diefenbash, M.; Harvey. J. N.; Schröder, D.; Schwarz, H. *Angew. Chem., Int. Ed.* **1998**, *37*, 829.

(26) Magnera, T. F.; David, D. E.; Michl, J. *J. Am. Chem. Soc.* **1987**, *109*, 936.

(27) Jackson, G. S.; White, F. M.; Hammill, C. L.; Clark, R. J.; Marshall, A. G. *J. Am. Chem. Soc.* **1997**, *119*, 7567.

(28) Hanmura, T.; Ichihashi, M.; Kondow, T. *J. Phys. Chem. A* **2002**, *106*, 11465.

(29) Koszinowski, K.; Schröder, D.; Schwarz, H. *J. Am. Chem. Soc.* **2003**, *125*, 3676.

(30) Koszinowski, K.; Schröder, D.; Schwarz, H. *Angew. Chem., Int. Ed.* **2004**, *43*, 121.

(31) Bröstrup, M.; Schröder, D.; Schwarz, H. *Organometallics* **1999**, *18*, 1939.

(32) Koszinowski, K.; Schröder, D.; Schwarz, H. *Organometallics* **2003**, *22*, 3809.

(33) Koszinowski, K.; Schröder, D.; Schwarz, H. *Organometallics* **2004**, *23*, 1132.

(34) Xia, F.; Chen, J.; Zeng, K.; Cao, Z. X. *Organometallic* **2005**, *24*, 1845.

(35) Fortunelli, A. *J. Mol. Struct. (THEOCHEM)* **1999**, *493*, 233.

(36) Basch, H.; Musaev, D. G.; Morokuma, K. *J. Mol. Struct. (THEOCHEM)* **2002**, *586*, 35.

(37) Amsterdam Density Functional (ADF) 2004, SCM, Theoretical Chemistry, Vrije Universiteit, Amsterdam, Netherlands (www.scm.com).

(38) Baerends, E. J.; Ellis, D. E.; Ros, P. *Chem. Phys.* **1973**, *2*, 41.

(39) Boerrigter, P. M.; te Velde, G.; Baerends, E. *J. Int. Quantum Chem.* **1988**, *33*, 87.

(40) te Velde, G.; Baerends, E. J. *J. Chem. Phys.* **1992**, *99*, 84.

(41) Pyykkö, P. *Chem. Rev.* **1988**, *88*, 563.

(42) Schwarz, H. *Angew. Chem., Int. Ed.* **2003**, *42*, 4442.

(43) Lenthe, E. V.; Baerends, E. J.; Snijders, J. G. *J. Chem. Phys.* **1993**, *99*, 4597.

(44) Lenthe, E. V.; Baerends, E. J.; Snijders, J. G. *J. Chem. Phys.* **1994**, *101*, 9783.

(45) Xia, F.; Chen, J.; Cao, Z. X. *Chem. Phys. Lett.* **2006**, *418*, 386.

(46) Minori, A.; Sayaka, M.; Takahito, N.; Kimihiko, H. *Chem. Phys.* **2005**, *311*, 129.

(47) Becke, A. D. *Phys. Rev. A* **1998**, *38*, 3098.

(48) Perdew, J. P. *Phys. Rev. B* **1986**, *33*, 8822.

(49) Lee, C.; Yang, W.; Parr, R. G. *Phys. Rev. B* **1988**, *37*, 785.

(50) Perdew, J. P.; Chevary, J. A.; Vosko, S.; Jackson, K. A.; Pederson, M. R.; Singh, D. J.; Fiolhais, C. *Phys. Rev. B* **1992**, *46*, 6671.

(51) Airola, M. B.; Morse, M. D. *J. Chem. Phys.* **2002**, *116*, 1313.

(52) Taylor, S.; Lemire, G. W.; Hamrick, Y.; Fu, Z. W.; Morse, M. D. *J. Chem. Phys.* **1988**, *89*, 5517.

(53) Spain, E. M.; Morse, M. D. *J. Chem. Phys.* **1992**, *97*, 4605.

(54) Bishea, G. A.; Marak, N.; Morse, M. D. *J. Chem. Phys.* **1991**, *95*, 5618.

(55) Bishea, G. A.; Morse, M. D. *Chem. Phys. Lett.* **1990**, *171*, 430.

(56) Balasubramanian, K. *J. Chem. Phys.* **1987**, *87*, 6573.

(57) Plattner, D. A. *Angew. Chem., Int. Ed.* **1999**, *38*, 82.

(58) Schröder, D.; Shaik, S.; Schwarz, H. *Acc. Chem. Res.* **2000**, *33*, 139.

(59) Schwarz, H. *Int. J. Mass Spectrom.* **2004**, *237*, 75.

(60) Dai, D. G.; Balasubramanian, K. *J. Chem. Phys.* **1994**, *100*, 4401.

(61) Harada, M.; Dexpert, H. *J. Chem. Phys.* **1996**, *100*, 565.

(62) Yuan, D. W.; Wang, Y.; Zeng, Z. *J. Chem. Phys.* **2005**, *122*, 114310.

(63) Schwarz, H. *Angew. Chem., Int. Ed. Engl.* **1991**, *30*, 820.

(64) Weisshaar, J. C. *Acc. Chem. Res.* **1993**, *26*, 213.

(65) Martinho Simöes, J. A.; Beauchamp, J. L. *Chem. Rev.* **1990**, *90*, 629.

(66) Ranasinghe, Y. A.; MacMahou, T. J.; Freiser, B. S. *J. Phys. Chem.* **1991**, *95*, 7721.

(67) Fukui, K. *J. Phys. Chem.* **1970**, *74*, 4161.

(68) Fukui, K. *Acc. Chem. Res.* **1981**, *14*, 363.

(69) Wang, H.; Carter, E. A. *J. Phys. Chem.* **1992**, *96*, 1197.

(70) Dediu, A. *Chem. Res.* **2000**, *100*, 543.

(71) Yanagisawa, S.; Tsuneda, T.; Hirao, K. *J. Comput. Chem.* **2001**, *22*, 1995.

(72) Dewar, M. J. S. *Bull. Soc. Chim. Fr.* **1951**, *18*, C71.

(73) Chatt, J.; Duncanson, L. A. *J. Chem. Soc.* **1953**, 2939.